P2.1 Combined use of headwind ramps and gradients based on LIDAR data in the alerting of low-level windshear/turbulence

P.W. Chan * and K.K. Hon
Hong Kong Observatory, Hong Kong, China

D.K. Shin
Korea Meteorological Administration, Republic of Korea

1. INTRODUCTION

The Hong Kong International Airport (HKIA) is situated in an area of complex terrain. To its south is the mountainous Lantau Island with peaks reaching 1000 m above mean sea level and valleys as low as 400 m in between. Terrain-disrupted airflow occurs inside and around HKIA for the prevailing winds of easterly through southerly to southwesterly. It accounts for the majority of the low-level windshear and turbulence reports from the pilots, i.e. occurring below a height of 1600 feet or within 3 nautical miles from the runway end. Such windshear and turbulence may be hazardous to the operation of the aircraft.

Since the majority of low-level windshear and turbulence in HKIA occurs in non-rainy situation, Doppler Light Detection And Ranging (LIDAR) systems have been introduced by the Hong Kong Observatory (HKO) to the airport for operational windshear alerting. A special scanning strategy, called the glide-path scan, has been devised to measure the headwind profiles along the glide paths with the simultaneous operation of the azimuth and elevation motors of the LIDAR scanners. Based on the headwind profiles, a sophisticated algorithm has been invented to automatically detect significant changes of the headwind, also called "windshear ramps" and issue windshear alerts. This glide-path scan windshear alerting algorithm (GLYGA in short) is the core of the LIDAR Windshear Alerting System in operation at HKIA. Technical details of GLYGA could be found in Shun and Chan (2008).

The terrain-disrupted airflow disturbances are transient and sporadic in nature due to their limited size (HKO, IFALPA and GAPAN, 2010). They may have a spatial scale of a few hundred metres only as shown in the LIDARs' velocity imageries. It would be difficult for the pilots to clearly differentiate between windshear and turbulence at times. At the moment, LIWAS is designed to capture significant windshear. As such, it may not be able to capture cases where the headwind fluctuation is less than the alerting threshold but is superimposed by turbulence. In this kind of situation, it may be advantageous to consider the gradient of headwind, instead of the magnitude of the headwind change itself.

The headwind gradient is considered in a windshear hazard factor for the alerting of microburst, which is also called F-factor (Hinton, 1993). F-factor is given below:

$$F = \frac{1}{g}\frac{d}{dt}U_x - \frac{w}{V_a}$$

where U_x is the headwind along the glide-path direction x, t is the time, w the vertical wind velocity, V_a the aircraft airspeed, and g the acceleration due to gravity. Windshear may be alerted if F-factor reaches ±0.105. In this paper, an alternative way of alerting terrain-induced windshear and turbulence would be considered, namely, the F-factor calculated based on the gradient of the LIDAR-measured headwind profile. The combination of F-factor and GLYGA alerts would also be discussed. However, two aspects of the calculation of LIDAR-based F-factor would not be considered in the present study, namely:

(a) the aircraft response to the headwind change would not be studied – for this purpose, the LIDAR headwind profile may need to be input into a flight simulator;
(b) the vertical acceleration term of F-factor is not calculated.

2. EXAMPLES OF F-FACTOR PROFILES

Examples of LIDAR headwind profiles and F-factor profiles are presented for some typical cases of windshear at HKIA. The first case is a shearline between background easterly and westerly over the sea to the west of HKIA on 17 April 2009. This shearline may occur as a result of both sea breeze during the day and terrain-disrupted airflow. As shown in Figure 1(a), the headwind change across the shearline is rather abrupt. An aircraft landing at the north runway of HKIA from the west at that time reported encountering of windshear with a headwind gain of 15 to 20 knots at a height of 500 feet. The F-factor reaches a maximum of about 0.35, which is also a rather large value. For a headwind change in the form of a step change, both GLYGA and F-factor give similar result.

Figure 1(b) corresponds to a case of fresh to strong southwesterly winds over the airport on 19 April 2009. The headwind profile shows rapid fluctuations, though the windshear ramps do not reach a magnitude of 14 knots or more. As a result, no GLYGA alert has been issued based on the LIDAR headwind profile in Figure 1(b). However, at 06:04 UTC, an aircraft landing at the north runway of HKIA

* *Corresponding author address:* P.W. Chan, Hong Kong Observatory, 134A Nathan Road, Hong Kong email: pwchan@hko.gov.hk

from the east reported the encountering of windshear of headwind gain of 18 knots and headwind loss of 10 knots at 700 feet. Such headwind changes are not substantiated by the LIDAR data. The turbulence may be taken as windshear by the pilot. Using F-factor, a peak as large as 0.25 is obtained at a distance of about 2.5 nautical miles away from the runway end. F-factor appears to be more effective in capturing the turbulent airflow, compared with identification of windshear ramps.

The third case occurs on 20 January 2009. Moderate to fresh easterly winds prevailed over the airport area, as typical in the spring time. Terrain-disrupted airflow appeared and an aircraft landing at the north runway from the west reported the encountering of headwind loss of 10 knots at 700 feet. The corresponding F-factor profile (Figure 1(c)) shows a peak at about 1 nautical mile away from the runway end, reaching a rather high value of 0.17. If an alerting threshold in the order of 0.15 – 0.2 is adopted, a windshear alert based on LIDAR F-factor may be issued and this would cause a false alarm.

The fourth case shows the occurrence of multiple "steps" in the headwind profile resulting in a windshear ramp. It occurs on 9 April 2007. The meteorological situation is similar to the first case, in which a shearline appeared at the western part of HKIA as a result of sea breeze and possibly terrain effect. However, different from the first case, the wind change across the shearline does not appear to be an abrupt jump, but in a series of smaller "steps" (Figure 1(d)). As GLYGA has an extension algorithm to take into account all the neighbouring wind changes (see Shun and Chan (2008) for details), a windshear alert would be issued for this situation. In fact, an aircraft landing at the north runway of HKIA from the west reported encountering windshear of headwind change of 20 knots. However, F-factor takes into account of local headwind gradients only (without considering the effect of aircraft response – see Section 1 of this paper), and as such the maximum value is in the order of 0.16. Taking into consideration the third case and the present case, the alerting threshold of LIDAR-based F-factor has to be chosen with caution in order to strike a good balance between hit rate and false alarm.

3. PERFORMANCE OF F-FACTOR IN CAPTURING WINDSHEAR

The use of F-factor and GLYGA in the alerting of low-level windshear is studied. As a start, only the pilot reports of significant windshear are considered. As the synoptic patterns are different in the Spring (January to April) and the Summer (May to September) seasons, seasonal performance of windshear alerting by F-factor and GLYGA is studied by considering the two mostly used arrival runway corridors of HKIA, namely, landing at the north runway from the west (07LA) and from the east (25RA). For GLYGA, the operational alerting threshold is used. For F-factor, the alerting threshold is varied in order to determine the optimal performance in the alerting of windshear.

Three different scenarios in the application of LIDARs for alerting windshear are adopted, namely, using F-factor only, considering the combination of F-factor *and* GLYGA (F *and* G), and considering the union of F-factor and GLYGA (F *or* G). It is apparent that the latest scenario would capture the largest number of pilot windshear reports. As benchmarks, the performance of F-factor with/without GLYGA is compared with that from the operational algorithms/service, namely, GLYGA only, Windshear and Turbulence Warning System (WTWS, which also includes the alerts from the other automatic windshear alerting algorithms such as ground-based anemometer algorithm, hilltop anemometer algorithm, and weather radar algorithm), and the overall windshear alerting service (including both WTWS and subjective windshear warnings issued by the aviation weather forecasters).

The performance is plotted in a diagram of percentage of detection (POD) vs. percentage of time with alerts (i.e. total alert duration divided by the period of time under consideration, expressed as a percentage). The performance diagrams for 2006 – 2009 are shown in Figure 2. It could be seen that, with the appropriate choice of F-factor threshold, the union of F-factor and GLYGA could achieve a POD larger than that by GLYGA alone by 10% or more. On one occasion (spring time, 25RA), it even surpasses the performance of the overall windshear alerting service. We are studying the cases over 25RA that are not captured by the overall windshear alerting service but with the union of F-factor and GLYGA.

4. STATISTICS OF LIDAR-BASED F-FACTOR

It would be interesting to see the statistical distribution of the LIDAR-based F-factor, which captures the wind climatology at HKIA. To the knowledge of the authors, the first LIDAR system at HKIA, installed in mid-2002, has the longest history of continuous operation in an airport in the world, when compared with similar Doppler LIDARs in other countries. Same as Section 3, the data between 2006 and 2009 are considered.

The LIDAR-based F-factor is essentially the radial velocity increment of adjacent range gates divided by the fixed range gate separation of 100 m. As such, the statistical distribution of F-factor may be modelled using the probability density function of wind speed increment following Castaing et al. (1990) and Bottcher et al. (2007).

Castaing et al. proposed that the increment distribution results from a superposition of Gaussian distributions in which the respective standard deviations are log-normally distributed. Control parameters of the log-normal function, namely the median and the variance, are then assumed by Bottcher et al. to depend on the mean wind speed, which is in turn described by the Weibull distribution well-known to the meteorological community. The distributions of wind speed increment at a number of positions along Runways 07LA and 25RA over the Spring and Summer seasons of 2006 to 2009 as measured by the LIDAR are shown in Figure 3. It is fitted with the theoretical distribution of Bottcher et al. in Figures 4(a) and (b), which is expressed as follows:

$$p(\Delta U) = \int_0^\infty d\sigma \int_0^\infty d\bar{u} \cdot \frac{k}{A^k} \bar{u}^{-k-1} e^{-(\frac{\bar{u}}{A})^k} \cdot \frac{1}{\sqrt{2\pi}\lambda\sigma} e^{-\frac{Ln^2(\frac{\sigma}{\sigma_0})}{2\lambda^2}} \cdot \frac{1}{\sqrt{2\pi}\sigma} e^{-\frac{(\Delta U)^2}{2\sigma^2}}$$

where ΔU is the wind speed increment, σ the Gaussian standard deviation, u-bar the mean wind speed, σ_0 and λ^2 the log-normal median and variance, k and A the shape and scale factor of the Weibull distribution respectively. As with Bottcher et al, the dependence of σ_0 on u-bar is taken to be linear and that of λ^2 on u-bar is considered weak and disregarded.

Under the logarithmic scale of Figures 4(a) and (b), marked deviation from Gaussian behaviour can be seen, which would otherwise assume the profile of an inverted parabola. Large velocity fluctuations, i.e. those at the tail-end of the distribution, occur at probabilities orders of magnitudes higher than as would be expected from normally-distributed behaviour. The heavy-tailed, non-Gaussian shape of the resulting distribution can be attributed to the intermittency of turbulence.

It could be seen from Figures 4(a) and (b) that the observed distribution could be fitted very well with the theoretical expression above, (a) both at a number of positions along Runway 07LA over the same time period, i.e. 2006 to 2009, and (b) at the same position on Runway 25RA over the four years considered individually. Statistical behaviour of wind increments also does not show significant variations either across the two runways under study or on an annual timeframe during the study period. It thus appears that a climatology of F-factor, hence possibly of windshear, could be established through long-term monitoring of wind speed increments. It is also envisaged that an analysis of intra-annual variation of F-factor statistics could shed light on the seasonal characteristics of windshear events occurring at HKIA.

5. CONCLUSIONS

The use of the gradient of LIDAR-measured headwind, also called the LIDAR-based F-factor, is considered in the alerting of windshear at HKIA. It turns out that the union of LIDAR-based F-factor and GLYGA could capture about 87 to 90% of windshear at the airport with an optimal choice of the alerting threshold of F-factor. Moreover, the F-factor is found to follow the statistical distribution previously reported for wind speed increment. The distribution takes on a tail-heavy, non-Gaussian shape, which is related to the intermittency of turbulence.

Future work would include the consideration of vertical acceleration term of F-factor and aircraft response. In particular, the LIDAR-based F-factor profile would be compared with that obtained from the aircraft data. Moreover, in view of the difficulty in differentiating between windshear and turbulence, the application of LIDAR-based F-factor in alerting of both windshear and turbulence would be considered, based on the pilot reports collected for HKIA.

References

Bottcher, F., St. Barth and J. Peinke, 2007: Small and large scale fluctuations in atmospheric wind speeds. *Stoch Environ Res Ris Assess,* 21:299–308

Castaing, B., Y. Gagne and E.J. Hopfinger, 1990: Velocity probability density functions of high Reynolds number turbulence. *Physica D* 46(2):177–200

Hinton, D. A., 1993: Airborne Derivation of Microburst Alerts from Ground-based Terminal Doppler Weather Radar Information – a Flight Evaluation. NASA Technical Memo. 108990, 32 pp.

Shun, C.M., and P.W. Chan, 2008: Applications of an infrared Doppler Lidar in detection of wind shear. *J. Atmos. Oceanic Technol.*, **25**, 637 – 655.

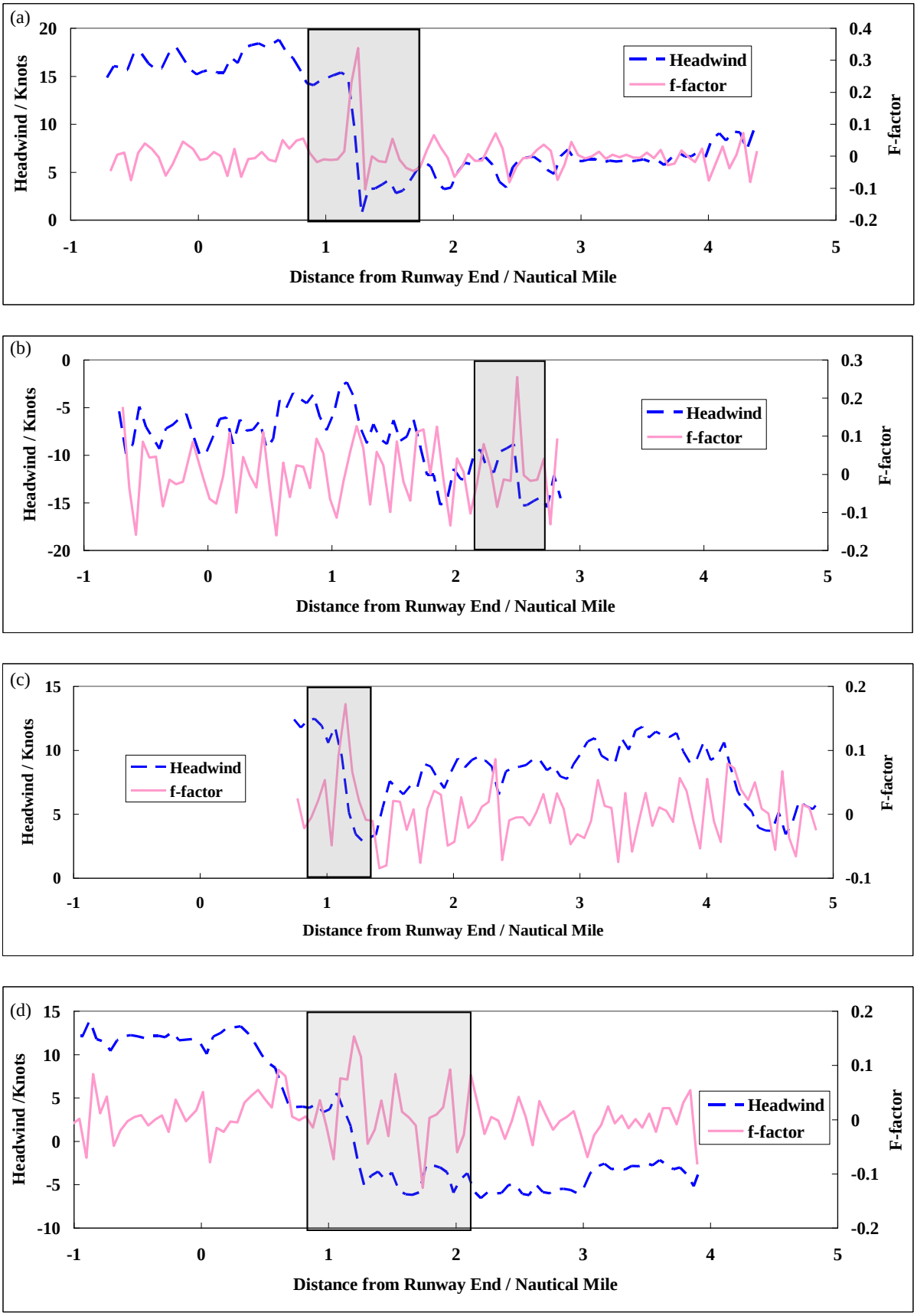

Fig. 1 LIDAR headwind and F-factor profiles for typical cases of windshear at HKIA: **(a)** 17 April 2009, **(b)** 19 April 2009, **(c)** 20 January 2009, and **(d)** 9 April 2007. Highlighted areas correspond to regions of disrupted airflow along the glide-path which possibly lead to the received windshear reports from pilots.

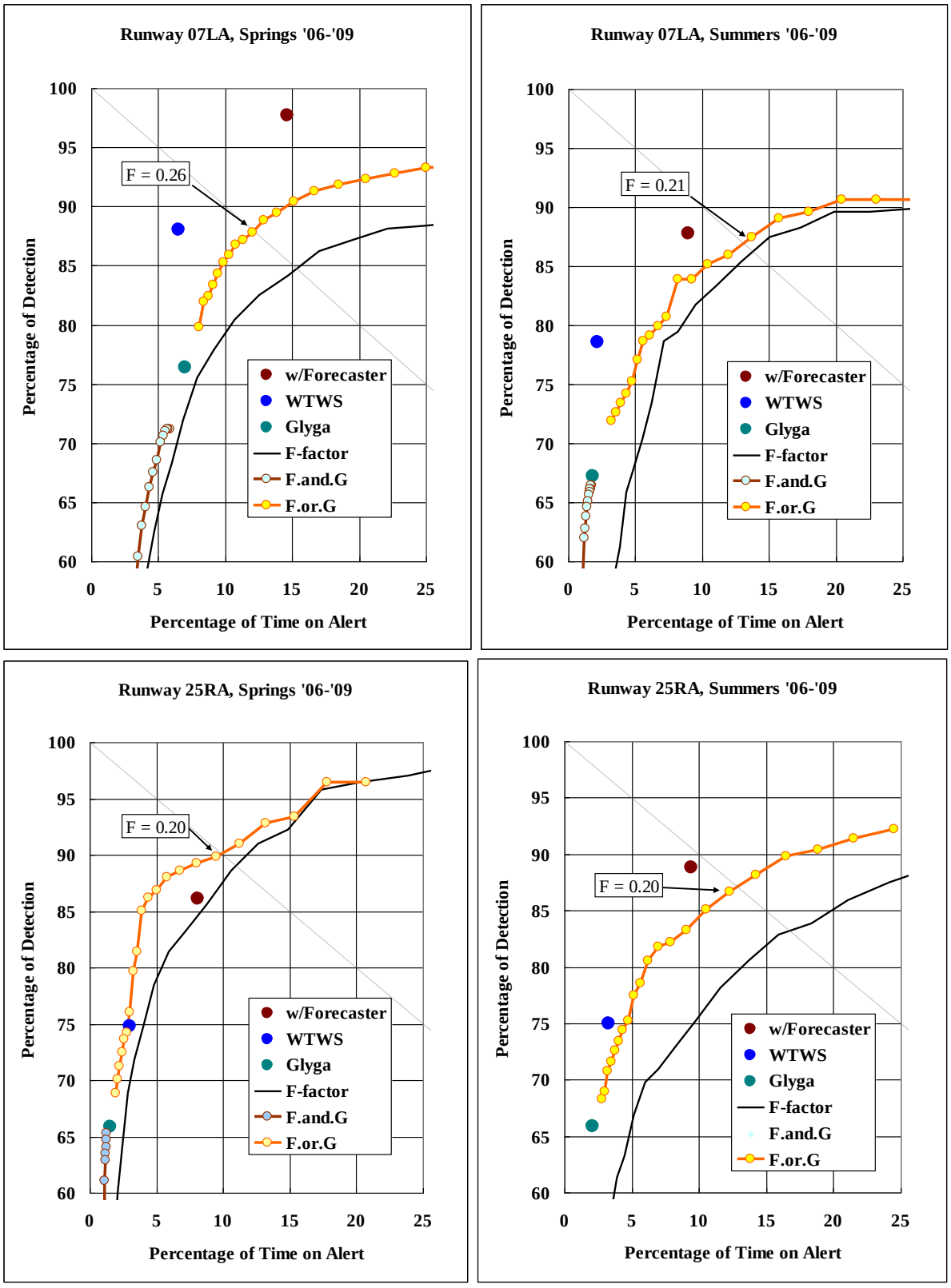

Fig. 2 Performance of windshear alerting algorithms on Runways 07LA and 25RA using logical intersection ("F.and.G") and union ("F.or.G") of "F-factor" and "GLYGA" over the Spring (Januray to April) and Summer (May to September) seasons of 2006 – 2009. "WTWS" refers to the currently operational Windshear and Turbulence Warning System. "w/Forecaster" refers to the overall windshear alerting service, including both WTWS and subjective windshear warnings issued by aviation weather forecasters. Lables refer to F-factor threshold values giving optimal performance to the "F.or.G" algorithm in the four different scenarios. Adjacent points on the "F.or.G" curves represent increments (towards the left) or decrements (towards the right) in threshold value in units of 0.1. The bottom left point on all four "F.or.G" curves refers to a threshold of 0.35.

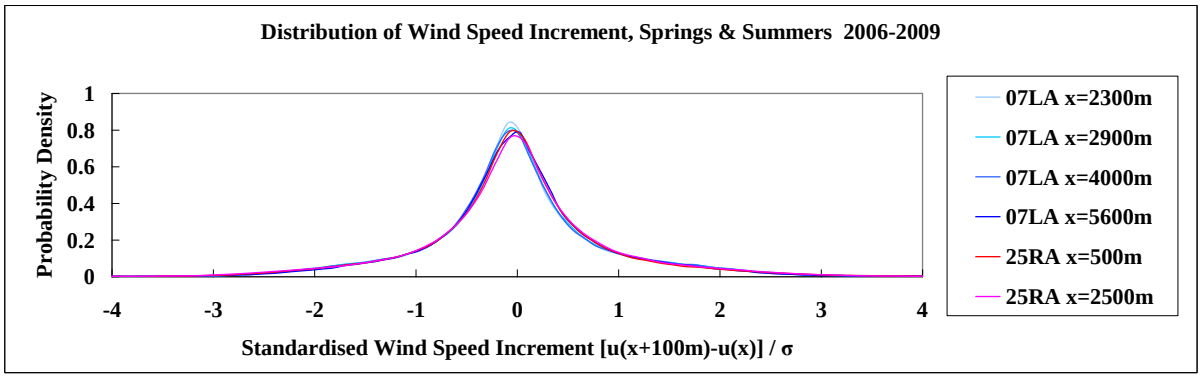

Fig. 3 Distribution of wind speed increment at a number of positions (*x*, measured from runway end) along Runway 07LA (*x* = 2300m, 2900m, 4000m and 5600m) and Runway 25RA (*x* = 500m and 2500m) compiled over the Spring and Summer seasons of 2006 – 2009 as measured by the LIDAR.

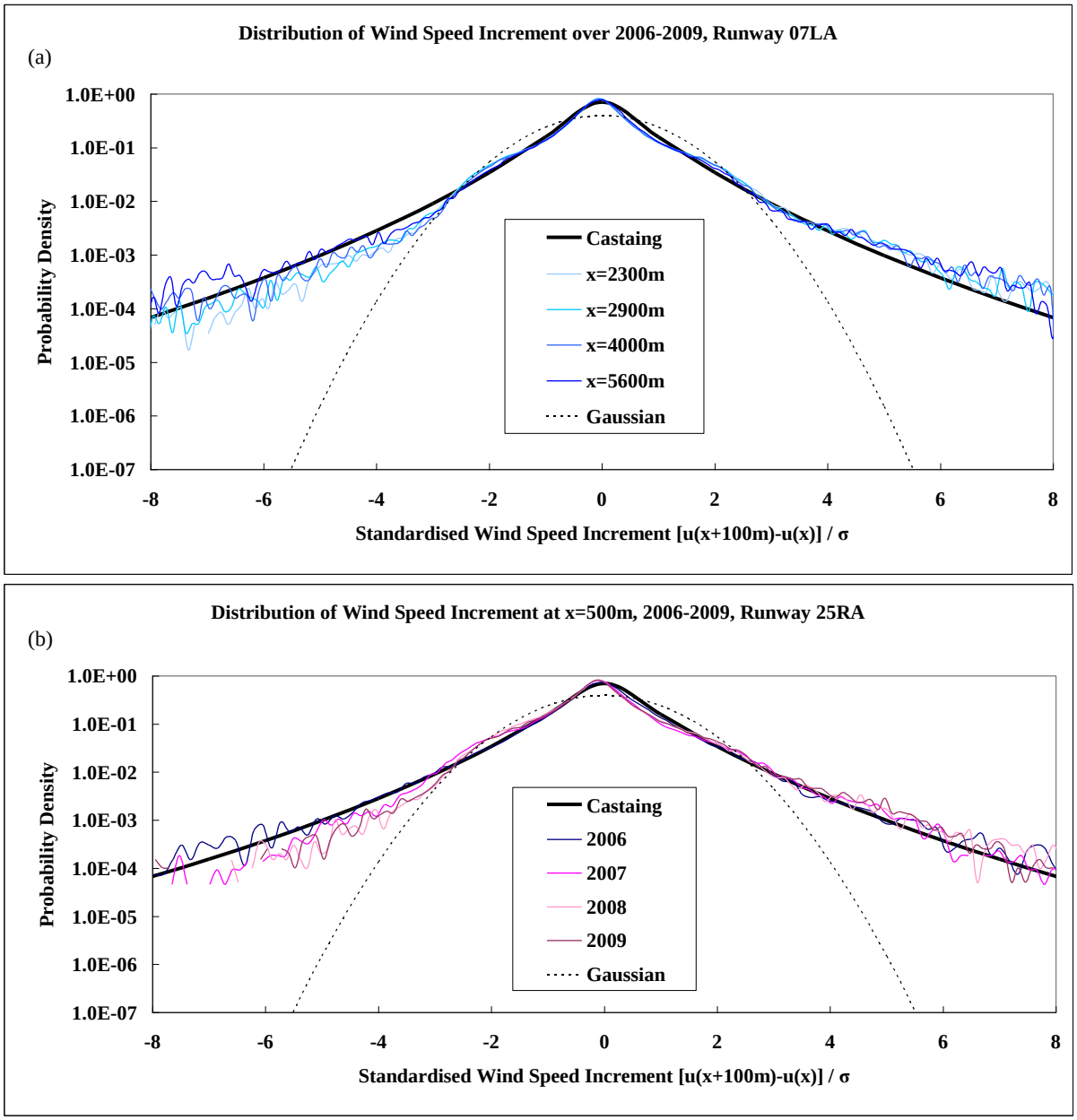

Fig. 4(a) Wind speed increment distribution, standardised and in logarithmic scale, at different positions along Runway 07LA over the Spring and Summer seasons of 2006 – 2009 and fitted with the theoretical expression by Bottcher et al. **(b)** Similar to (a), but using data at a fixed position (x=500m) on Runway 25RA with the four years considered separately. The Gaussian function in both plots, also standardised for comparison, highlights the departure from normally-distributed behaviour.